

# Development of Intertwined Infills to Improve Multi-Material Interfacial Bond Strength

Irfan Mustafa and Tsz-Ho Kwok\*

Department of Mechanical, Industrial and Aerospace Engineering  
Concordia University  
Montreal, QC H3G 1M8, Canada

*Recently the availability of various materials and ongoing research in developing advanced systems for multi-material additive manufacturing (MMAM) have opened doors for innovation in functional products. One major concern of MMAM is the strength at the interface between materials. This paper hypothesizes overlapping and interlacing materials to enhance the bonding strength. To test this hypothesis, we need a computer-aided manufacturing (CAM) tool that can process the overlapped material regions. However, existing computational tools lack key multi-material design processing features and have certain limitations in making full use of the material information, which restricts the testing of our hypothesis. Therefore, this research also develops a new MMAM slicing framework that efficiently identifies the boundaries for materials to develop different advanced features. By modifying a ray tracing technology, we develop layered depth material images (LDMI) to process the material information from computer-aided design (CAD) models for slicing and process planning. Each sample point in the LDMI has associated material and geometric properties that are used to identify the multi-material regions. Based on the material information in each slice, interlocking joint (T-Joint) and interlacing infill are generated in the regions with multiple materials. Tensile tests have been performed to verify the enhancement of mechanical properties by the use of overlapping and interlacing materials.*

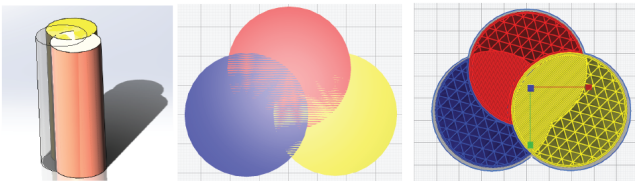
## 1 Introduction

Additive manufacturing (AM) technology utilizes a layer-by-layer stacking method to produce real three-dimensional (3D) structures from the input geometry. Since their introduction more than 20 years, AM systems have been used in a variety of applications. These applications have ranged from conventional products to highly complex design models required in advanced applications. The geometric freedom and the free-form manufacturing technology enables AM to fabricate complex structures with accurate material deposition capability at the specified positions defined in the design domain or computer-aided design (CAD)

model. Research advances in AM and the availability of new materials have unlocked a new world of endless possibilities with customization in additive manufacturing that lead to complex multi-material structures [1, 2, 3, 4]. A multi-material object is a solid model composed of varying material properties within a specified domain inside the geometry. Availability of diverse materials with different properties is one of the main reason for innovation happening in the development of multi-material structures. This allows overcoming the existing single material AM limitations for the development of functional objects. Multi-material additive manufacturing (MMAM) has a lot of benefits and that is why MMAM technology is innovating rapidly to fabricate advanced products that can meet today's demand. With all the advantages of 3D printing (complex design, low cost and customized performance etc.), multiple materials can provide additional flexibility of using desired materials for desired mechanical performance. Such a mechanical behaviour is highly desirable for example in 3D printing of tailor-made implants or soft robotics due to multiple requirements of varying stiffness and shorter production times [5, 6].

The printing of discrete multi-material objects is a technically difficult process, but an economically favourable manufacturing method, and it provides additional functionality and flexibility [7]. In the case of multi-material fused filament fabrication (FFF), the inter-facial bond at the joint between different materials is developed based on the fusion of one material into other materials, and the strength of the bond is highly dependent on the compatibility between two materials. This lack of fusion is the main reason for parts breakage at the interface of materials. Considerable research and analytical studies have been conducted to analyze the effect of interface on the overall strength of the part. To improve the strength of inter-facial bond, different interlocking joints were developed and analyzed [8]. This shows that a macroscopic interface interlocking or material fusion can improve the strength of the inter-facial bond. Different other strategies have also been implemented like an application of chemicals and redistribution of materials during post-processing to soften the material. However, these strategies still have the joint weaker than the materials themselves.

\*Email: tszho.kwok@concordia.ca



SOLIDWORKS 2019 Geometry      Cura 4.4.1 Input Geometry      Cura 4.4.1 Toolpath

Fig. 1. Current Slicers Overlapping Materials Handling Issues

It is observed that the nature often intertwines materials to strengthen the overall structure, like plants. Human does the same too; for example, in the manufacturing of composite materials, different interlacing patterns of fibres in the composite sandwich panel have resulted in significant improvement of mechanical property and other properties like energy absorption [9]. Interlacing fibres in clothing fabric has multiple advantages including enhancing the durability and the resilience of a fabric [10]. Many AM processes, e.g., FFF, are like building and placing fibers, and the deposition way of these manufacturing technologies has a direct effect on the mechanical properties of the fabricated part. Based on these observations on how the nature and human do to enhance mechanical properties, we hypothesize that overlapping and even interlacing materials at the interface will increase the bonding strength in MMAM. To test this hypothesis, one way is to expand the interface of different materials to a small overlapping region and generate the infill within the region with both the materials. Although overlapping various parts can be designed in the CAD phase, the generation of the interlaced infill and the toolpath needs to be done in the slicers. The capabilities of currently existing slicers are very limited in terms of the processing of a material information in a multi-material model. In-case of a multi-material model with overlapping geometries as shown in Fig. 1, these commercially available slicers randomly assign materials to overlapping geometry. Due to this reason these slicers cannot develop interlocking features in 3d prints which can considerably enhance the mechanical properties of a multi-material structure.

This technology gap shows that the current computer-aided manufacturing (CAM) tools cannot make full use of material properties for MMAM. As such, we have to develop an advanced computational tool to process multi-material models. A ray representation – layered-depth images (LDI) [11] – is employed here, since it is a compact format containing volumetric information, and thus it can perform many tasks quickly such as collision detection, haptic rendering, and Boolean operations. Making use of the materials specified in the CAD model, we develop a new format named layered-depth material images (LDMI) to encode the material information in the LDI sample points. The sample points encoded with material information can tell whether a region of a layer has a single material or multiple materials. Multi-material infills can be generated for the multi-material regions, and contours can be constructed at the interface be-

tween different regions too. Our contributions are summarized as follows.

1. A new computational tool is developed for MMAM, which can take multi-material CAD models as input and use the material information in the slicing and tool-path planning.
2. Knowing the material distribution in different regions, infill interlacing can be realized in the multi-material regions.
3. Tensile test results show that interlaced infills increase the bond strength and outperform the T-joint interlocking. The fracture even happens outside the interface area, meaning that the bonding is at least as strong as the materials.

Besides a dog-bone model is used for the tensile tests, various multi-material models with overlapping regions are tested with the present LDMI tool. The experimental results show that LDMI can also handle the regions having more than two materials. This paper generates tool-paths as the result based on the FFF technology, but the methodology can be extended to other MMAM processes.

The rest of the paper is organized as follows. Section 2 reviews the related works. Section 3 presents the methodology and the implementation details. The experimental results are presented in Section 5. Finally, section 6 concludes the paper with future works.

## 2 Related Work

Our research involves the computer-aided design and manufacturing of MMAM and has a focus on the enhancement of bonding between materials, so a brief review is done related to these fields.

### 2.1 Multi-material additive manufacturing

Different AM technologies are being used for MMAM [1], and each has its own properties. For example, Polyjet uses the ink-jetting technology to jet different materials [12], selective laser melting (SLM) melts different powders together [13], digital light processing (DLP) changes materials by swapping the vats [14]. Among all these technologies, the most popular and easily accessed one is probably the FFF method [15, 16]. This is because it is clean and can add more materials by using more nozzles. MMAM technologies can be used to improve part performance by varying material compositions, which are not achievable by conventional manufacturing processes, and this opens multiple opportunities for design, functionality, and cost-effective high-value products [17], especially in medical and dental where high performance is required with desirable properties for biomedical applications. Despite much research has been done in this area, there are still many challenges, e.g., bonding between dissimilar materials, overall low interfacial bonding, and multi-material data processing from CAD to CAM [1, 18].

## 2.2 Process planning for multi-material printing

Computer graphics researchers both in academia and in the industry are contributing significantly to developing modelling and designing strategies for MMAM using various schemes such as spatial subdivisions schemes including voxels [19] and surfels [20]. However, there are some issues inherent in the current AM that has have halted the progress towards MMAM. Even the most advanced CAM tools for AM are based on conventional geometrical and processes in AM [21]. Due to this, current MMAM slicers cannot utilize all the material information available in the CAD to the full extent [1]. In the past, multiple approaches have been tried to overcome the constraints in handling multi-material products. One of the approach that is used to represent the multi-material model is a multi-CAD system [22]. This multi-CAD system is a set of STL models from available CAD modelers with the solid information replaced by the material index. It requires users to specify the material information and the printing properties for each STL model separately, which adds certain complications to MMAM. Recently, a digital material design framework is proposed to find a proper material distribution by separating the whole domain into blocks and filling them up based on the tensor values [23].

## 2.3 Interface and bonding between materials

Ribeiro et al. [8] has analyzed the effect of different kind of mechanical interlocking joints on the strength of the multi-materials interface. They compared different materials and different interlocking joints (T-Shape, Dovetail Shape and U Shape) for analyzing the adhesion and interlocking strength. It was concluded that the strength of the interface joint is much more dependent on the macroscopic structure of the interface (mechanical interlock) than the material compatibility. Interface joints play a key role in the performance of multi-material part and has been analyzed a lot in the past. Previously various techniques have been tested to develop a strong inter-facial bond between materials of different compatibility. Rossing et al. [24] presented a technique to control the bonding between flexible material like silicone and thermoplastics through mechanical interlocking. Bonding strength between silicone and thermoplastics was improved drastically using a hybrid fabrication process. Another research [25] analyzed the adhesive behaviour between materials in each layer and it was concluded that various printing parameters like print orientation can affect the strength of the interface. Therefore, the strength at the interface can be improved by controlling these parameters. Lumpe et al. [26] also showed that strength at the material interface is directly related to the materials and design of the interface. Some structures can even result in 20% increased strength using new multi-material structures designing algorithms. However, directly developing interlocking features like T-joints and lattice structures at the interface in CAD model is a cumbersome and difficult process that requires a lot of time.

## 3 Methodology

Our proposed approach for MMAM is based on the LDI [27], which is developed on top of ray-tracing technology, as it is scalable to generate binary images for DLP printing. LDI represents a model  $H$  by a 2D array of pixels viewed from a single camera with parallel rays that pass through the centers of pixels. Ray tracing shoots a ray from the pixels to intersect the solid model obtaining a set of sample points, and then it determines the In/Out for every sample point if the rays are going in to or coming out from the solid model. Each LDI pixel stores the depth values of the intersection points between the pixel and the surface of the input geometry  $H$ . Compared to other slicing technologies like contour slicing and voxelization, ray tracing is computationally efficient for detecting small features like material overlapping and interlocking joints in complex AM structures [28]). Other than this, the related geometrical computations can be accelerated by modern graphics hardware equipped with a Graphics Processing Unit (GPU) by processing the pixels in parallel. Compared to LDI sampling, other existing methods may fail [29] or give poor performance [30] when the layer-complexity of an input model is high. Applying the LDI technique here can potentially solve one of the biggest challenges in multi-material AM to manufacture objects with multiple materials.

Our proposed LDMI framework is shown in Fig. 2. Initially, we read an input CAD design as an AMF file and build a material library. This library stores the materials used in the model and gives an index to each material. These images are then applied to develop sticks, which are the contours of the model or between different materials. These contours can be utilized in the generation of interlocking patterns at the multi-material interface. Interlacing infill can also be realized within the multi-material regions bounded by the contours. The problem considered in this research is defined as follows. Suppose a multi-material object  $H \in \mathbf{R}^3$  is defined by  $n$  materials in the CAD geometry. If a region is filled with material  $i$ , then the specific material region is called  $O_i$ . Therefore, the input multi-material model can be defined as  $H = \{O_1 \cup \dots \cup O_n\}$ . The overlapping region between different materials is defined by  $O_{m,n} = O_m \cap O_n$ . Each of the single-material and multi-material regions will be identified and defined separately in LDMI. This is done by binding the material information from the CAD model onto the LDMI sample points, and they are used for the identification of material regions. The technical details are presented in the following sections.

### 3.1 Sampling with material information

A key component in this process was to transfer the material information available on the CAD model to the LDI sample points efficiently utilizing graphics hardware, and this section will briefly present the technique for binding material information on the LDMI binary samples. Modelling the multi-material interface based on LDMI representation is dependent on the input material information specified in the CAD model. In the LDMI program, we used AMF file to

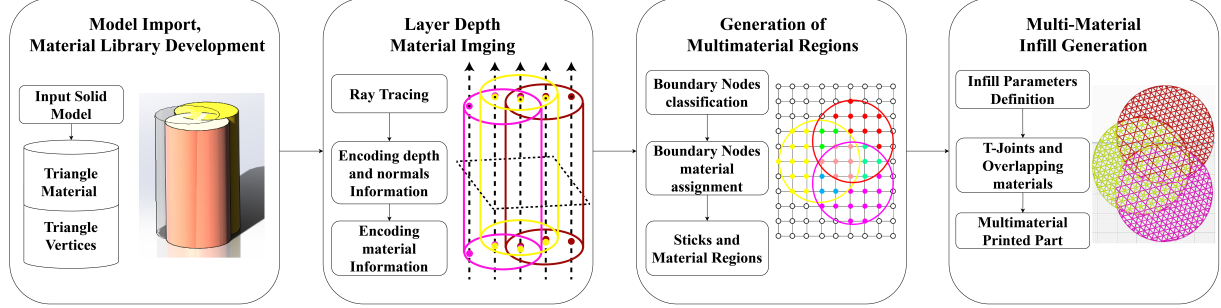


Fig. 2. LDMI framework for modeling multi-material interface

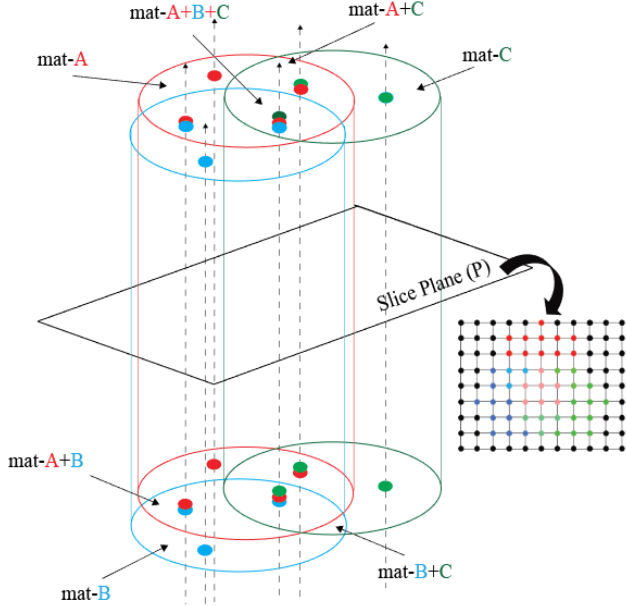


Fig. 3. LDMI sample points on a ray.

take a multi-material polygonal mesh as an input. The *AMF* file format is used because it is currently the most widely adopted file format for the processing of multi-material models. The material data is stored for each volume of the model defined by a set of triangular faces.

The mesh representation is converted to LDMI through ray tracing as shown in Fig. 3. The sampling of ray tracing can be done by GPU rendering. Rendering a model in the 3D space is to project and convert its triangles into a raster image located at the screen. This rasterization fills up the image pixels based on the shapes of the triangles as well as their properties like colors. For a particular viewing direction, there are some triangles in the front and some in the back. To avoid multiple passes of rasterization, we make use of the color parameter to store the coordinate as well, so that the position of all points can be directly retrieved by the rendering results at once. A color can be defined by four floating points:  $(r, g, b, a)$ , for the red, green, blue, and alpha (transparent) channels. We use the one ( $r$ ) to store the depth value ( $d$ ) of a point, which is sufficient to locate the 3D position. This is because the viewing direction and the image plane

is known. The viewing direction is set to the Z-axis, assuming it as the printing direction, and the image plane is located at the build plate. Another one ( $g$ ) is used to store the material index ( $m$ ), which is corresponding to a particular material in the material library. The rest two ( $b, a$ ) are used to store the first two components of the normal at the point  $(n_x, n_y)$ , which are used to determine if the ray is going into or leaving the model at the point. Just the two components are enough, because the third one can be calculated by them, e.g.,  $n_z = 1 - n_x - n_y$ . In other words, a LDMI sample point is actually represented as  $(d, m, n_x, n_y)$ , and they are stored and sorted in the ray of corresponding pixel at which they are located. After binding material information on every sample, we obtain LDMI samples as a list of 2D textures shown with Red and Green colors as shown in the second block in Fig. 2. Note that the sample points are from the top and bottom surfaces of the cylinders.

### 3.2 Slicing for multiple materials

This section will present the slicing algorithm that use the LDMI sample points to determine the material composition for different regions at a layer. For each layer of a given height, a plane parallel to the LDMI is placed at the height to intersect with all the rays of LDMI. The plane is also a 2D image having its nodes aligned with the rays, so its resolution is the resolution of LDMI minus one. The nodes are first classified with the materials, and then the boundaries between the materials can be constructed.

#### 3.2.1 Material Assignment to Nodes

Classification of nodes as an In/Out node and material assignment can be accomplished by comparing a node with the sample points. First, we can classify the status of nodes as an in/out node of whole input solid model  $H$  by comparing it with the depth and the normal of sample points. Second, for all the In-nodes, we can assign a material value to these nodes. Suppose if on a ray we have only 2 samples, a node is lying in between an In-sample of material A and an Out-sample of A, then we assign material A to the node. Subsequently, If we have 4 samples on a ray, then the material encoding program assigns the material value for the nodes according to the material present on those 4 sam-

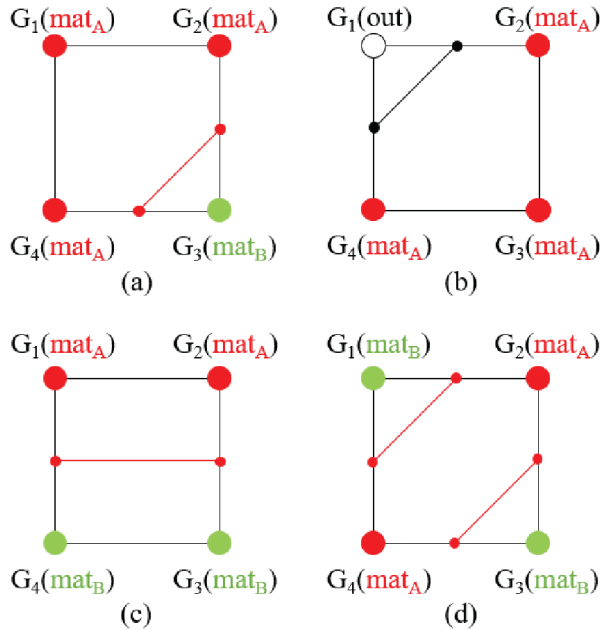


Fig. 4. Some examples in constructing sticks in each cell. The sticks (in red) between two materials form internal boundary separating two material regions, and the ones (in black) form external boundary.

ples. This material assignment on gridnodes is completely processed using GPU. Fig. 3 shows the same approach that any node lying inside an overlapping material region will get a unique index value based on the materials forming the overlap. Using this efficient parallel approach for searching and assignment of material, we develop an efficient data-set of grid nodes defining just the boundary and material for every material  $m$  inside  $H$ . This approach generates a pool of nodes with material status.

### 3.2.2 Development of Multi-material Contours

After assigning the status and material to every node, the next step is to classify the boundary of the material region and for this, we first need to identify the boundary cells. A cell can be classified as a boundary cell if at least one node in the cell has a different material status. Some examples of the boundary cells are shown in Fig. 4. If red nodes represent material  $A$  and green nodes represent material  $B$ , then we can build a stick to connect the edges where their two endpoints have different materials. The boundary can be further classified as internal or external depending if it is a boundary between different materials or external of the model. This process will be repeated for every material region. Using this material status on nodes, we connect the edges of a cell to develop a stick  $S$  and these sticks belonging to same material are joined with each other to develop contours for that material.

### 3.3 Modeling of Material Interfaces

One important aspect of multi-material geometry is the boundary region that is located at the interface between different materials and how to develop interlocking features to enhance the mechanical strength of such and inter-facial joint. This section presents our proposed approach to develop a T-joint and a mixed infill in the regions with material overlap.

#### 3.3.1 T-joint

Ribeiro et al. [8] concluded that the T-joint interlocking pattern can improve the mechanical performance at the interface. While they modeled the T-joints explicitly using CAD software, here we show that with the present LDMI framework, they can be generated automatically in the slicing without changing the CAD model. First of all, the length for every T-joint is specified by input property of  $T - joint\ size$  and depending on the desired number of the T-joint, sticks at a specific location are replaced with new sticks developed for T-joint. Fig. 5 shows an example if we require *two* T-joints and the total number of sticks is *six*, then a shift of two Sticks is applied to get equidistant two T-joints. Shift value varies for the opposite *green* material at the interface to develop interlocking T-joints and also to enclose the T-joints developed by *red* material. Every contour developed by LDMI program is constructed by small sticks which are shown in Fig. 5. Using the input value for *Number of the T - joints* and *T - joint size*, the desired percentage of interlocking at the inter-facial joint can be controlled. Size of T-joint is controlled by the length of the main vertical leg of the T-joint. For each new T-joint, new sticks are developed by rotating the old sticks at a specified angle accordingly to form a T-joint shape. For each leg of a T-joint, a new stick is generated and the old sticks are replaced by these newly developed sticks forming a T-joint. A similar procedure is repeated for second material forming the interface *green*. Contrary to first *red* material, T-joints for second material *green* are developed in the form of a cavity to enclose the joints developed by the first material *red*. This cavity forms the T-joints for the second material forming the interface. Fig. 5 represents the visual output of the strategy we followed to develop the T-Joint. Note that the sticks of a T-joint can be preset, and whenever a T-joint is needed, this preset can simply replace an original stick based on its orientation and direction. In this way, the inclusion of T-joints can be done implicitly regardless of the shape of the CAD models.

#### 3.3.2 Intertwined infills

After developing contours for each material in the previous steps next step in LDMI program is to develop the triangular infill for every contour. Overall the contours generated for input geometry  $H$  can be classified according to two material regions: single-material region and multi-material region. For a single-material region, infill is generated for a single material, and for a multi-material region, infill is generated with every material in that region. Here, we present how to generate intertwined infills for the multi-material re-

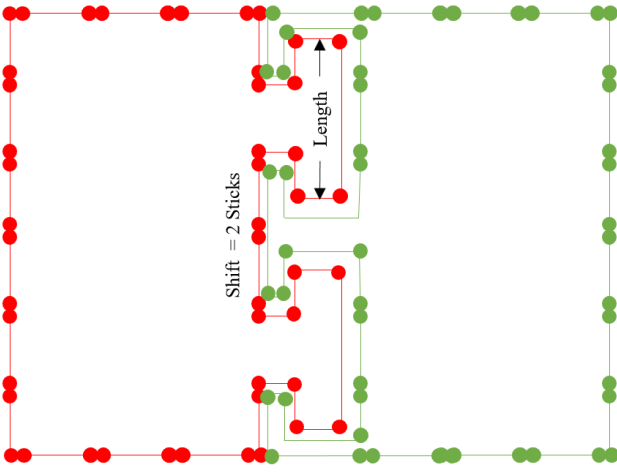


Fig. 5. Development of T-Joints at Red and Green Material Interface. Size of the T-Joint is length of one vertical leg of T-joint

gion. As a first step to the generation of multi-material infill, infill properties are specified for every material forming the multi-material region. An important property is the *Infill Ratio* which allows to specify ratios between (0%-100%) for the overall infill. This can be translated to the ratio of each material, like if there are two materials, then each is half of the total ratio. These infill ratios are used to calculate the *Infill Line Distance* which basically is a multiple of infill ratio and specifies the distance between the infill lines of a material. For each material forming the contour there is an additional property *Infill Shift* that gives and additional shift to the infill lines of the material. It ensures that infill lines for every material are shifted relative to all other materials forming the contour which creates an interlacing effect, as infill generated for a material is shifted and developed on top of the infill lines generated for other materials. To further enhance the interlacing effect, the LDMI program generates an infill to print alternate material on top of each other for every layer. Specifically, in overlapping region, the infill lines are interlaced between layers as well by printing them in alternate ways such as: Layer-1 ( $M_A$  at bottom, and  $M_B$  at top) and Layer-2 ( $M_A$  at top,  $M_B$  at bottom). This creates an additional interlacing effect between different materials in the Z-axis to improve compatibility and strength at the interface joint. Here, we use the triangular infill, in which the lines are generated at three angles (0, 60, 120) for each material which are connected using the Greedy approach for the shortest material printing path. Till now FFF multi-material additive manufacturing has not been able to achieve a mixed transition from one material to another. Utilizing the boundary information in the overlap region, we print mixed infill by printing different materials within the same domain with different infill ratios and other printing properties.

#### 4 Results and Discussion

The proposed LDMI slicing framework was implemented as a C++ program with Microsoft Visual Studio

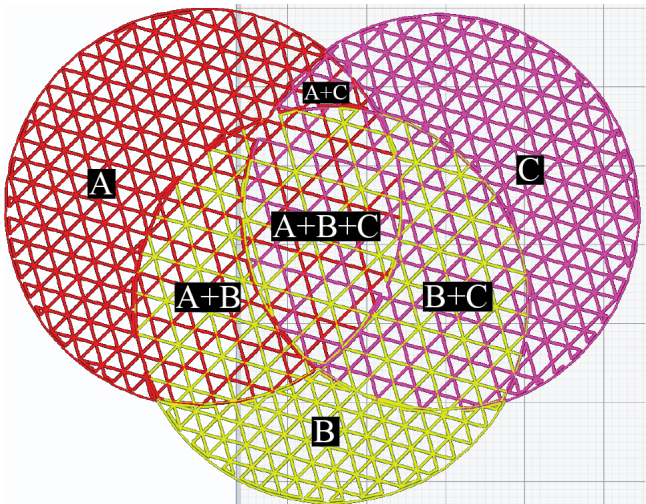


Fig. 6. Cura 4.4.1 visualization of the tool-path for the three overlapping cylinders.

2017. All the examples shown here are tested with Intel CORE i5 7th Generation with 8GM RAM and Nvidia GeForce 920M graphics card.

#### 4.1 Interlacing Infill

In first test case of our research we developed intertwined infill for three overlapping cylinders and the G-Code visualization using *Cura* – 4.4.1 is shown in Fig. 6. For this test case LDMI program efficiently processed each of total seven material regions and developed 3d printing tool-path for three single material and four multi-material infill regions. Tool-path development is an independent process for all the material regions and this gives much more control to achieve desired mechanical properties in a multi-material structure. It is important to highlight that in our proposed LDMI framework interlacing infill was obtained without any modification in the input solid model  $H$ .

In Fig. 6 small solid circles in intertwined infill regions shows that how infill of different material overlap and intersect with each other. Moreover LDMI program develops a tool-path in such a way that there is no definite boundary/infill wall between different material regions. Interlacing different materials in infill in this way plays a key role in the smooth transitioning of mechanical properties in the multi-material structure. Moreover, in LDMI developed 3d printing tool-path, alternate printing of material in the Z-axis ensures even stronger inter-facial bond and smooth transition of mechanical properties in a Z-direction as well.

LDMI program can efficiently detect the materials, and different colors in Fig. 6 represent different material regions. In this three-cylinder model, there are in total seven material regions with different material combinations. The regions could have different number of material according to the desired mechanical properties.  $A$ ,  $B$ , and  $C$  are single material regions with single material infill whereas  $A+B$ ,  $A+C$ ,  $B+C$ , and  $A+B+C$  are multi-material regions with intertwined infill. In-case of a material region such as  $A+B+C$ , infill ratio is evenly divided among the each of the material

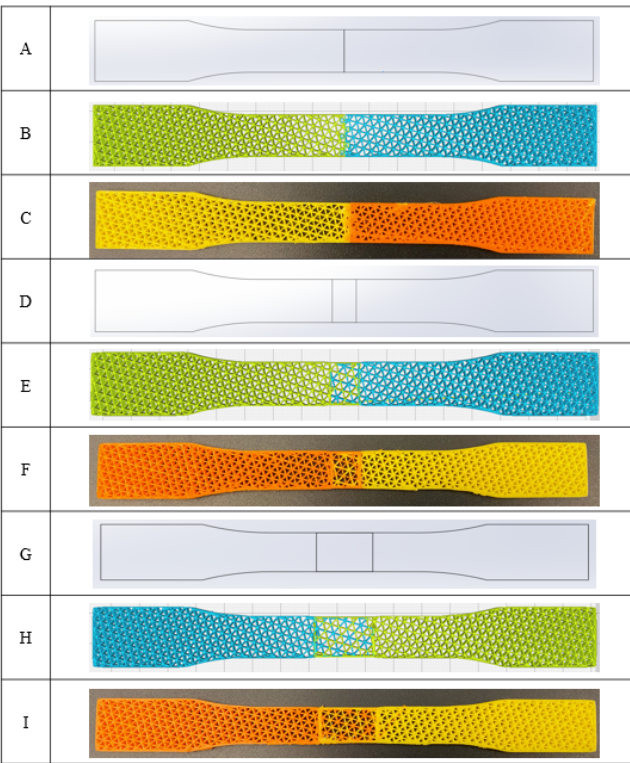


Fig. 7. A,B,C: T-joint samples. D,E,F: 10(mm) overlap configuration. G,H,I: 20(mm) overlap configuration

forming the material region. Moreover the suing the property of *infill – ratio* infill lines of a material is shifted relative to other material and because of this the infill lines of material A are aligned with the infill lines of B in A + B multi-material region.

Similarly, all other material regions have a degree of homogeneity for infill lines. This makes the extruded materials to diffuse into each other which allows for gradual transition materials in between different material regions. In the interlaced infill for a region of overlapping materials, different materials are overlapped with each other and are extruded on top of each other as circled in Fig. 6. Infill triangles developed for interlaced infill have edges made up of three materials which creates an interlocking effect in between three materials in a triangular design. Other infill patterns like *Cross* and *Gyroid* can be applied to the material overlapping regions too. Overall these results also clearly demonstrates that LDMI program can handle more than two materials.

#### 4.2 Tensile test

In our research we initially hypothesized that an interlaced infill at the interfacial joint can enhance the mechanical properties of a multi-material structure. To test our hypothesis, we conducted tensile tests on four different interfacial joint configurations of the dog-bone samples. These configurations include Simple interfacial joint, T-joint, 10mm intertwined infill and 20mm intertwined infill. In Simple interfacial joint, there is no interlocking mechanism and is set as a base case for for comparison and to assess the improvement

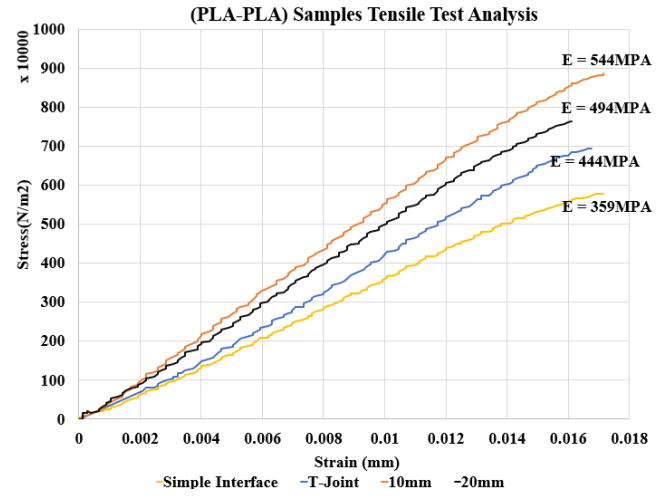


Fig. 8. Tensile test analysis results

in the mechanical properties due to T-joint and intertwined infill. Dog bone samples for these configurations are shown in Fig. 7. All the dog bones samples were modeled following *ASTM – D63* design guidelines and were 3D printed using *Ultimaker – 3* dual extruder FFF 3d printer with PLA material. Tensile tests were performed using *Mark – 10* instrument. Fig. 8 shows the stress/strain graph for the elastic region until the ultimate stress point, and Table 1 summarizes the ultimate stress, Young modulus, and the improvement of different samples. For the dog-bone samples printed with the simple interfaical joint configuration, the observed ultimate tensile stress value was about 3.58MPA. For the samples with interlocking features of T-Joint the observed ultimate tensile stress value was about 6.85MPA where as for intertwined infill of 10mm and 20mm the observed ultimate tensile stress value was about 8.88MPA and 7.65MPA respectively. During comparison we found that ultimate stress value for simple interfacial joint was increased by about 20.03%, 53.35% and 32.12% in T-joint, 10mm and 20mm dog-bone samples respectively. These results clearly show that interlocking features developed in LDMI program like the T-joint and the intertwined can considerable enhance mechanical properties in a multi-material structure.

By comparing the elastic modulus for 10mm intertwined infill and 20mm intertwined infill, we observed that the elastic modulus of the 10mm interfacial joint configuration was 9.19% higher than the elastic modulus of the 20mm interfacial joint configuration. Similar trend was also observed in the ultimate stress values with a 13.8% difference. From this comparison, we inferred that the increasing the size of intertwined infill region does not result in enhancement of the mechanical properties. Therefore, for a certain size of intertwined infill we can achieve best mechanical properties in multi-material structure.

Overall we tested twelve samples: three for each joint configuration, and all the three samples of each configuration performed similarly. Fig. 9 shows the fractured locations for all the configurations. The T-joint interlocking configuration fractured at the joint, whereas the two intertwined

Joint Configuration	Ultimate Stress (MPA)	% Improvement
Simple Joint	5.79	—
T-Joint	6.95	20.03
10mm Intertwined	8.88	53.36
20mm Intertwined	7.65	32.12

Table 1. Comparison of intertwined infill joint configurations with simple interfacial joint configuration.

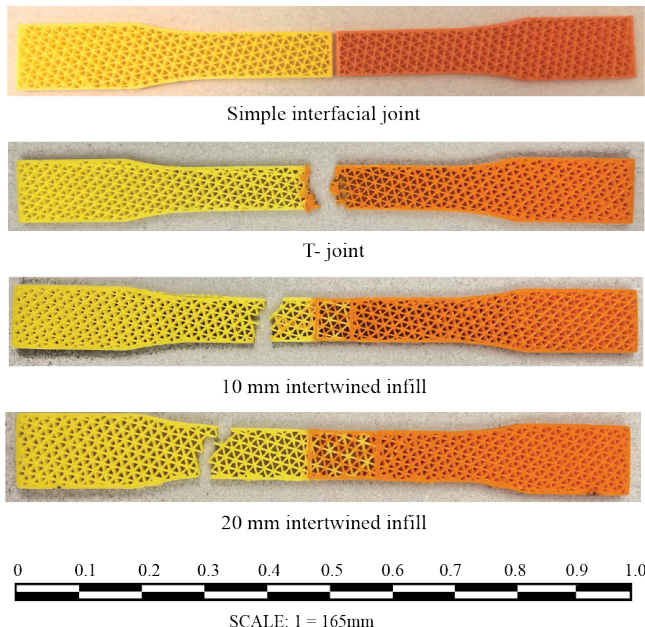


Fig. 9. Fractured Test Samples. Simple Interface joint fractured right at the interface similar to T-joint whereas intertwined infill interfacial joints did not break at joint.

infill configurations fractured at least 10mm away from the joint. After analysing the fracture locations, we concluded that the interfacial bond developed by the interlacing infills was stronger than the T-joint configuration.

These results and the data validates our initial hypothesis highlight the motivation for our work. Currently, existing slicers do not have any capability to handle any material overlap in the solid model. LDMI program develops interlocking features at inter-facial joint, which can be a cumbersome procedure in CAD. As all the post-processing for developing interlocking patterns and interlace infill is happening in LDMI program, so this creates an additional benefit of using LDMI as a plugin for existing CAM systems.

#### 4.3 Different materials

In the previous section, we compared dog-bone samples with different interfacial-joint configuration, for this purpose we printed all the samples with (*Orange – PLA* and *Yellow – PLA*) material combination. However, it does not mean that LDMI program works only for the same mate-

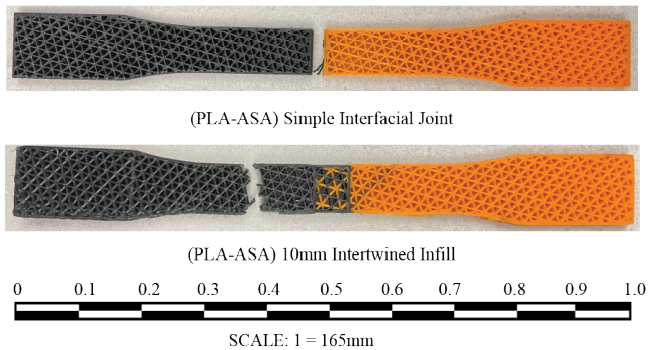


Fig. 10. Multi-material dog bone samples

rial or a single material. To demonstrate the capability of processing different materials, we printed dog-bone samples (*PLA – PTEG* and *PLA – ASA*) material combination as show in Fig. 10. After analyzing the tensile test results of different interfacial joint configurations we observed that 10mm intertwined infill joint configuration achieved best mechanical properties hence we hypothesized that even for the material combination of (*PLA – ASA*) dog-bone samples with 10mm overlap will have the strongest interfacial bond. Due to this reason in this even for different materials we compared only 10mm intertwined infill dog-bone samples. The tensile test results of the dog-bone samples with (*PLA – ASA*) material combination resulted in the elastic modulus value of about *354MPA* with an ultimate stress value of about *5.85MPA* where as for the same material combination and simple interfacial joint configuration we observed the elastic modulus value of about *345.6MPA* and an ultimate stress value of about *3.24MPA*. This is *33.79%* improvement in value of ultimate stress. This shows that intertwined infill can also enhance the mechanical properties of a multi-material structure printed with incompatible materials.

## 5 Conclusions and Future Work

In summary, we have presented a novel multi-material additive manufacturing slicer developed using LDMI methodology which generates and layered depth material images and multi-material infills. Using our proposed research solid models can be printed by using any multi-material FFF printer with multiple extruders. Our work provides a solid foundation on how to use multi-material information present in the CAD to intelligently develop the T-joint interlocking or the intertwined infill in CAM process without any extra process in the CAD. While most of the current existing additive manufacturing slicers have multiple limitations specifically in detection of the overlapping region to develop infill mix for the gradual transition of material properties, our proposed framework offers a promising tool for defining the printing parameters and printing each material independently in a single model. We have printed dog-bone samples and conducted tensile tests to analyses the strength of the infill mix. The printed samples and the results from tensile tests show considerable improvement in printing a clear interface between two material and using T-joint inter-

locking or interlacing infills. By analyzing the tensile test results of dog-bone samples featuring the intertwined infill configuration, it appears that in other MMAM processes, the use of intertwined infill can improve the mechanical properties of a multi-material part. In one of the previous research [31] selective laser melting was used for 3d printing of a multi-material part and it was observed that the hardness value at the interfacial joint, ranged between those of the two materials forming the transition zone. Similarly in other research [32] authors reported the same behaviour with the dimensional variation of the interfacial region in a multi-material structure. In our future work, we plan to extend our present work to functionally graded infill and other infill patterns following the principles of LDIMI. We also plan to extend our LDIMI framework for DLP printing in the future as we already have developed LDIMI that can be used to generate images for DLP printing.

## Acknowledgements

This paper acknowledges the support of the Natural Sciences & Engineering Research Council of Canada (NSERC) grant #RGPIN-2017-06707.

## References

- [1] Vaezi, M., Chianrabutra, S., Mellor, B., and Yang, S., 2013. “Multiple material additive manufacturing—part 1: a review: this review paper covers a decade of research on multiple material additive manufacturing technologies which can produce complex geometry parts with different materials”. *Virtual and Physical Prototyping*, **8**(1), pp. 19–50.
- [2] Bandyopadhyay, A., and Heer, B., 2018. “Additive manufacturing of multi-material structures”. *Materials Science and Engineering: R: Reports*, **129**, pp. 1–16.
- [3] Sreeramagiri, P., Bhagavatam, A., Ramakrishnan, A., Alrehaili, H., and Dinda, G. P., 2020. “design and development of a high-performance N-based superalloy WSU 150 for additive manufacturing”. *Journal of Materials Science & Technology*, **47**, pp. 20–28.
- [4] Brackett, D., Ashcroft, I., and Hague, R., 2011. “Topology optimization for additive manufacturing”. In Proceedings of the solid freeform fabrication symposium, Austin, TX, Vol. 1, pp. 348–362.
- [5] Meisel, N., and Williams, C., 2015. “An investigation of key design for additive manufacturing constraints in multimaterial three-dimensional printing”. *Journal of Mechanical Design*, **137**(11).
- [6] Tibbits, S., 2014. “4D printing: multi-material shape change”. *Architectural Design*, **84**(1), pp. 116–121.
- [7] Salonitis, K., Pandremenos, J., Paralikas, J., and Chrysosolouris, G., 2009. “Multifunctional materials used in automotive industry: A critical review”. In *Engineering Against Fracture*. Springer, pp. 59–70.
- [8] Ribeiro, M., Carneiro, O. S., and da Silva, A. F., 2019. “Interface geometries in 3D multi-material prints by fused filament fabrication”. *Rapid Prototyping Journal*, **25**(1), pp. 38–46.
- [9] Van Hoa, S., Duc Hoang, M., and Simpson, J., 2017. “Manufacturing procedure to make flat thermoplastic composite laminates by automated fibre placement and their mechanical properties”. *Journal of Thermoplastic Composite Materials*, **30**(12), pp. 1693–1712.
- [10] Nawab, Y., Hamdani, S. T. A., and Shaker, K., 2017. *Structural textile design: interlacing and interlooping*. CRC Press.
- [11] Huang, P., Wang, C. C. L., and Chen, Y., 2014. “Algorithms for layered manufacturing in image space”, book chapter, asme advances in computers and information in engineering research”. *ASME Advances in Computers and Information in Engineering Research*.
- [12] Sitthi-Amorn, P., Ramos, J. E., Wangy, Y., Kwan, J., Lan, J., Wang, W., and Matusik, W., 2015. “Multifab: a machine vision assisted platform for multi-material 3D printing”. *ACM Transactions on Graphics (TOG)*, **34**(4), pp. 1–11.
- [13] Demir, A. G., and Previtali, B., 2017. “Multi-material selective laser melting of fe/al-12si components”. *Manufacturing Letters*, **11**, pp. 8 – 11.
- [14] Matte, C.-D., Pearson, M., Trottier-Cournoyer, F., Dafoe, A., and Kwok, T. H., 2019. “Automated storage and active cleaning for multi-material digital-light-processing printer”. *Rapid Prototyping Journal*, **25**(5), pp. 864 – 874.
- [15] Brennan, R., Turcu, S., Hall, A., Hagh, N., and Safari, A., 2003. “Fabrication of electroceramic components by layered manufacturing (LM)”. *Ferroelectrics*, **293**(1), pp. 3–17.
- [16] Roach, D. J., Hamel, C. M., Dunn, C. K., Johnson, M. V., Kuang, X., and Qi, H. J., 2019. “The  $m^4$  3D printer: A multi-material multi-method additive manufacturing platform for future 3D printed structures”. *Additive Manufacturing*, **29**, p. 100819.
- [17] Deng, D., Kwok, T.-H., and Chen, Y., 2017. “Four-Dimensional Printing: Design and Fabrication of Smooth Curved Surface Using Controlled Self-Folding”. *Journal of Mechanical Design*, **139**(8), 06. 081702.
- [18] Han, D., and Lee, H., 2020. “Recent advances in multi-material additive manufacturing: methods and applications”. *Current Opinion in Chemical Engineering*, **28**, pp. 158–166.
- [19] Aremu, A. O., Brennan-Craddock, J., Panesar, A., Ashcroft, I., Hague, R. J., Wildman, R. D., and Tuck, C., 2017. “A voxel-based method of constructing and skinning conformal and functionally graded lattice structures suitable for additive manufacturing”. *Additive Manufacturing*, **13**, pp. 1–13.
- [20] Jones, M. W., Baerentzen, J. A., and Sramek, M., 2006. “3D distance fields: A survey of techniques and applications”. *IEEE Transactions on visualization and Computer Graphics*, **12**(4), pp. 581–599.
- [21] Muller, P., Hascoet, J.-Y., and Mognol, P., 2014. “Tool-paths for additive manufacturing of functionally graded

- materials (FGM) parts”. *Rapid Prototyping Journal*.
- [22] Qu, X., and Langrana, N. A., 2001. “A system approach in extrusion-based multi-material cad 313”. In International Solid Freeform Fabrication Symposium.
- [23] Leung, Y.-S., Kwok, T.-H., Mao, H., and Chen, Y., 2019. “Digital material design using tensor-based error diffusion for additive manufacturing”. *Computer-Aided Design*, **114**, pp. 224 – 235.
- [24] Rossing, L., Scharff, R. B., Chömpff, B., Wang, C. C. L., and Doubrovski, E. L., 2020. “Bonding between silicones and thermoplastics using 3d printed mechanical interlocking”. *Materials & Design*, **186**, p. 108254.
- [25] Vu, I. Q., Bass, L. B., Williams, C. B., and Dillard, D. A., 2018. “Characterizing the effect of print orientation on interface integrity of multi-material jetting additive manufacturing”. *Additive Manufacturing*, **22**, pp. 447–461.
- [26] Lumpe, T. S., Mueller, J., and Shea, K., 2019. “Tensile properties of multi-material interfaces in 3D printed parts”. *Materials & Design*, **162**, pp. 1–9.
- [27] Wang, C. C. L., Leung, Y.-S., and Chen, Y., 2010. “Solid modeling of polyhedral objects by layered depth-normal images on the GPU”. *Computer-Aided Design*, **42**(6), pp. 535–544.
- [28] Kwok, T.-H., 2019. “Comparing slicing technologies for digital light processing printing”. *Journal of Computing and Information Science in Engineering*, **19**(4).
- [29] Heidelberger, B., Teschner, M., and Gross, M., 2003. “Real-time volumetric intersections of deforming objects”. In Vision, modeling, and visualization 2003, AKA, pp. 461–468.
- [30] Liu, F., Huang, M.-C., Liu, X.-H., and Wu, E.-H., 2010. “Freepipe: a programmable parallel rendering architecture for efficient multi-fragment effects”. In Proceedings of the 2010 ACM SIGGRAPH symposium on Interactive 3D Graphics and Games, pp. 75–82.
- [31] Wei, C., Li, L., Zhang, X., and Chueh, Y.-H., 2018. “3d printing of multiple metallic materials via modified selective laser melting”. *CIRP Annals*, **67**(1), pp. 245–248.
- [32] Zhang, Y., and Bandyopadhyay, A., 2018. “Direct fabrication of compositionally graded ti-al<sub>2</sub>O<sub>3</sub> multi-material structures using laser engineered net shaping”. *Additive Manufacturing*, **21**, pp. 104–111.